 CMC, vol.32, no.3, pp.177-200, 2012

Design Optimization of Composite Cylindrical Shells under Uncertainty

B. Kriegesmann[1], R. Rolfes[1], E. L. Jansen[1], I. Elishakoff[2]
C. Hühne[3] and A. Kling[3]

Abstract: Four different approaches for the design of axially compressed cylindrical shells are presented, namely (1) the knockdown factor (KDF) concept, (2) the single perturbation load approach, (3) a probabilistic design procedure and (4) the convex anti-optimization approach. The different design approaches take the imperfection sensitivity and the scatter of input parameters into account differently. In this paper, the design of a composite cylinder is optimized considering the ply angles as design variables. The KDF concept provides a very conservative design load and in addition an imperfection sensitive design, whereas the other approaches lead to a significantly less conservative design load and to a less imperfection sensitive design configuration. The ways in which imperfection sensitivity is treated by the different approaches and how these influence the optimal design configuration is discussed.

Keywords: buckling, cylindrical shells, design optimization, composites.

1 Introduction

In contrast to beams and plates, the load carrying capability of axially compressed cylindrical shells is influenced by deviations from the perfect structure like geometric imperfections and imperfect boundary conditions. This induces difficulties when designing shells, since imperfections are unknown *a priori*. Design guidelines like NASA SP-8007 [NASA (1968)] propose knockdown factors (KDF) to account for uncertainties. These KDFs are based on a multitude of experimental tests that were carried out in the 1960s. For modern shells, these KDFs turned out to be overly conservative [Arbocz and Starnes (2002)]. Furthermore, NASA

[1] Leibniz University Hannover, Institute of Structural Analysis, Germany
[2] Florida Atlantic University, Department of Ocean and Mechanical Engineering, USA
[3] German Aerospace Center (DLR), Institute of Composite Structures and Adaptive Systems, Germany

SP-8007 is intended for metal shells and does not consider the additional design variability that occurs in composite shells, due to the laminate setup. Hence, several approaches have been followed in the past to find a physically based design procedure that is applicable to anisotropic shells, that both includes the effect of imperfections and simultaneously is less conservative than NASA SP-8007. A broad overview and summary of the effort that has been spent on phenomenon of buckling of cylindrical shells is given in [Elishakoff (2012)].

Beside the knockdown factor concept, three different, alternate design approaches are presented within this work: a probabilistic design procedure according to Elishakoff (1983)[see also Elishakof (1998); Elishakoff (2000); Elishakoff et al (2001, 1987); Arbocz and Stam (2004); Arbocz and Hol (1991)], that was recently extended by Kriegesmann et al (2011), [see also Kriegesmann et al (2010b)], the convex anti-optimization concept, which was introduced by Elishakof and Ohsaki (2010) and the deterministic single perturbation load approach by Hühne et al (2008), [see also Hühne (2006)]. Within the latter concept, a physically motivated lower bound is determined without knowing the actual imperfections. No imperfection pattern measurement is needed to determine the design load of a shell. The probabilistic method as well as the anti-optimization method account for input parameters based on measurements. In the current work the scatter in geometry, boundary conditions, material parameters and wall-thickness is taken into account.

It must be stressed that different design procedures do not only lead to different design loads, but also to different optimal designs. Zimmermann (1992) optimized the design of composite cylinders by maximizing the linear buckling load of the perfect shell, by varying fiber orientations and the number of plies. Hühne et al (2008); Hühne (2006) showed that maximizing the buckling load of an imperfect shell leads to a different laminate setup than for the perfect shell.

In the current work the design loads given by different design approaches are maximized by optimizing the laminate setup of the composite shells considered. In particular, the relation between the way in which imperfection sensitivity is treated and the optimal design configuration will be addressed, and the influence of the way in which the randomness of the input parameters is included on the optimal design configuration will be investigated.

2 Scatter in Input Parameters

For a probabilistic design approach and for the anti-optimization method measurement data are required for the type of shell that is designed. To this end, measurements on ten nominally identical composite cylinders are conducted. These have been manufactured and tested at DLR in Degenhardt et al (2010). The cylinders have nominal a radius of 250mm, a length of 500mm and a wall-thickness of 0.5mm. The laminate setup of the tested cylinders is [±24°, ±41°].

2.1 Traditional Imperfections

The geometric imperfections reducing the buckling load strongly are the most investigated imperfection, therefore, commonly denoted as "traditional" ones (see e.g. Hilburger and Starnes (2002) and Kriegesmann et al (2010a)). They have been measured using an optical measurement system (see Degenhardt et al (2010)). In order to parameterize the two dimensional field (1) that describes the geometric imperfections, which is periodic in circumferential direction, a Fourier series (1) is used.

$$\bar{W}(x,y) = t \sum_{k=0}^{n_1} \sum_{l=0}^{n_2} \bar{\xi}_{kl} \cos \frac{k\pi x}{L} \cos\left(\frac{ly}{R} - \bar{\varphi}_{kl}\right) \tag{1}$$

The Fourier coefficients $\bar{\xi}_{kl}$ and $\bar{\varphi}_{kl}$ characterize the scatter of geometry, L, R and t are length, radius and wall-thickness of the shell, respectively, x and y the coordinates in axial and circumferential direction. The indices k and l equal the number of axial half waves and circumferential full waves. For the shells considered, the upper bounds of the summation indices k and l are chosen to be $n_1 = 10$ and $n_2 = 20$. Hence, the total of $11 \cdot 21 \cdot 2 = 462$ parameters describe the scatter of the shell surface. In order to reduce the number of parameters, the reducing Mahalanobis transformation (2) or modified principal component analysis is used, respectively. For this, all Fourier coefficients are subsumed in the vector $\mathbf{x}$.

$$\mathbf{x} = \mathbf{B}\mathbf{z} + \mu \quad \text{and} \quad \mathbf{z} = \mathbf{B}^{-1}(\mathbf{x} - \mu) \tag{2}$$

The vector μ is the mean vector of $\mathbf{x}$ and the matrix $\mathbf{B}$ is a root of the covariance matrix Σ of $\mathbf{x}$, which is determined from the spectral decomposition of Σ. Via this transformation, the random vector $\mathbf{X}$ is transformed to vector $\mathbf{Z}$, which has uncorrelated entries with a mean value of zero and a standard deviation of one. The vector $\mathbf{Z}$ always has a length smaller than the number of measurements μ and Σ are estimated from. Hence, in the current example the 462 Fourier coefficients subsumed in the random vector $\mathbf{X}$ are transformed to only nine uncorrelated parameters, subsumed in the vector $\mathbf{Z}$. For more information the reader can refer to Kriegesmann et al (2011).

The geometric imperfections of one test cylinder are exemplarily shown in Figure 1.

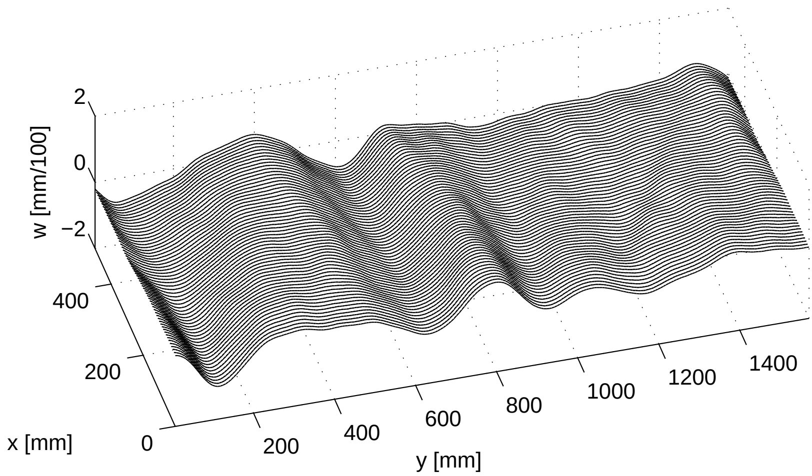

Figure 1: Geometric imperfections of one cylinder

2.2 Non-Traditional Imperfections

The term non-traditional imperfection refers to all kind of deviations from the perfect shell excluding geometric imperfections [Arbocz and Starnes (2002)]. In the following, an imperfect load application, deviations of wall-thickness t and scattering of material parameters are considered. Mean value values and standard deviations of all non-traditional imperfections considered are summarized in Table 1.

Table 1: Mean value values and standard deviations of non-traditional imperfections

	E_{11}	E_{22}	G_{12}	t	θ
Mean value	157362MPa	10095Mpa	5321MPa	0.48mm	0.012°
Standard deviation	3763MPa	415MPa	59MPa	0.0115mm	0.0027°

The distribution of material properties are obtained from a series of coupon tests [Degenhardt et al (2010)]. The Poisson's ration was assumed to be constant $\nu 12 = 0.277$. Orf (2008) found that for the considered shells, the spatial variation of the wall-thickness variation within one shell does not need to be taken into account. Instead, only the average wall-thickness is regarded as a scattering parameter.

An inclination of the load introduction plane was applied to the shells during tests, which was caused by the test setup. Because of the significant influence of the resulting bending moment on the buckling load, the inclination is determined indirectly for each shell. For this, finite element simulations have been performed in which the measured geometric imperfections as well as the measured wall thicknesses have been applied. The inclination angle θ was varied and thereby for each shell the value of θ has been determined, which yields the same buckling load as the experiment. These values serve as data set for the inclination angle θ. In this case the inclination covers also further imperfections. For a detailed description of this procedure see Kriegesmann et al (2011). It is worth mentioning that even though an inclination angle of about 0.01° seems to be very small, the difference between finite element simulations with and without considering inclination ranges from 10% to 29% for the cylinders considered. As shown, the inclination angle has a strong influence on the buckling load, therefore further research is needed to determine its size more precisely.

3 Design Procedures for Cylindrical Shells

In this section, the different approaches for the design of axially compressed cylindrical shells are summarized.

3.1 Knockdown Factor

Weingarten et al (1965) formulated a lower bound of buckling load as a function of the ratio of radius and wall-thickness R/t, based on compiled experimental data available at that time. This lower bound given in (3) has been adopted by the guideline NASA SP-8007 [NASA (1968)]:

$$\gamma = 1 - 0.901\left(1 - e^{-\phi}\right) \text{ with } \phi = \frac{1}{16}\sqrt{\frac{R}{t}} \tag{3}$$

Other guidelines propose KDF depending on the initial imperfections. For negligibly small imperfections and $L/R \leq 0.95\sqrt{R/t}$, the ECCS 56 [ECCS (1988)] gives a knockdown factor γ according to the following formulas:

$$\gamma = \frac{0.83}{\sqrt{1 + 0.01R/t}} \text{ for } \frac{R}{t} < 212 \tag{4}$$

$$\gamma = \frac{0.70}{\sqrt{1 + 0.01R/t}} \text{ for } \frac{R}{t} > 212 \tag{5}$$

If the largest dimple depth in the initial imperfection pattern exceeds a critical value, the KDF is further decreased. The same holds for Eurocode 3 [General

Rules (2002)] and the old German guideline DIN 18800 [Stahlbauten (1990)]. For these two guidelines, also the material strength is considered in the determination of a KDF. DIN 18800 furthermore considers the length of a cylinder. The KDFs suggested by the guidelines mentioned are plotted in Figure 3 and Figure 2 as functions of *R*/*t*.

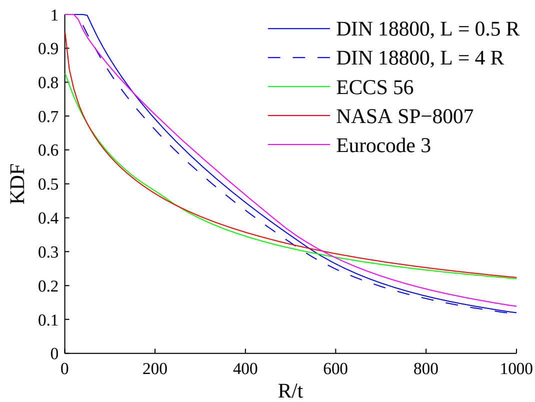

Figure 2: Knockdown factors (assuming highest quality class for Eurocode 3 and DIN 18800)

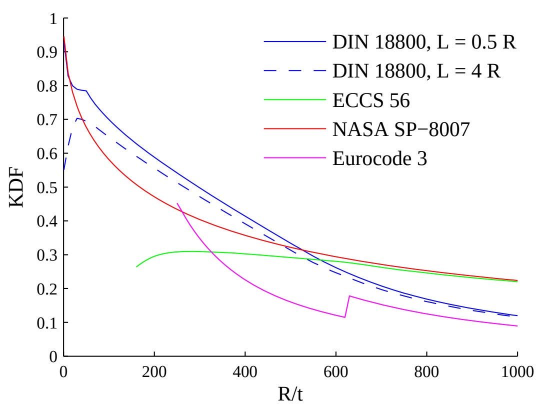

Figure 3: Knockdown factors for an imperfection amplitude of *t*

For Figure 2 the maximum depth of initial dimples was assumed to be zero, while for Figure 3 the maximum dimple depth was taken to equal the wall-thickness. The material properties of common steel are used for Eurocode 3 and DIN 18800.

Within Eurocode 3 shells are subdivided into three categories depending on their deepest initial dimple and the KDF is determined with respect to the category. For the example considered, the category changes for a ratio $R/t \approx 600$, which explains the jump in the KDF curve of Eurocode 3 in Figure 3.

The cylinders considered in this study have a ratio R/t of 500. Hence, the KDFs given by the different guidelines have values of about 0.3 (except Eurocode 3 for large imperfections). In the following, only NASA SP-8007 will be used for comparison. Treating the composite shell like metal shells leads to a KDF of $\gamma = 0.322$ according to equation (3). NASA SP-8007 also gives a lower bound for orthotropic shell, where the exponent ϕ is determined by:

$$\phi = \frac{1}{29.8}\sqrt{\frac{R}{t^*}} \text{ with } t^* = \sqrt[4]{\frac{D_{11}D_{22}}{A_{11}A_{22}}} \tag{6}$$

Here, A_{11}, A_{22}, D_{11} and D_{22} are the entries of the ABD-matrix. DeVries (2009) suggested to use the unified formulation (7) for composite shells.

$$\phi = \frac{1}{29.8}\sqrt{\frac{R}{t^*}} = \frac{1}{16}\sqrt{\frac{R}{\sqrt{12}t^*}} = \frac{1}{16}\sqrt{\frac{R}{t^+}} \text{ with } t^+ = \sqrt{12}t^* = \sqrt{12}\sqrt[4]{\frac{D_{11}D_{22}}{A_{11}A_{22}}} \tag{7}$$

This way, the KDF is determined with respect to the laminate setup. However, for each laminate setup $[\pm\alpha, \pm\beta]$ with arbitrary ply angles α and β the equivalent thickness t^+ is always $t^+ = t$ and hence, the KDF is $\gamma = 0.322$ independent from α and β.

3.2 Single Perturbation Load Approach

Hühne et al (2008), Hühne (2006) proposed a deterministic approach to find a physically reasonable lower bound of buckling load, which is referred to as "single buckle approach" (SBA) [see e.g. Huhne et al (2008) and Kriegsmann et al (2010a)], "single perturbation load approach" [see Elishakoff et al (2011)] or "lateral perturbation load approach" in the literature. For the single perturbation load approach a lateral perturbation load is applied to the cylinder within the buckling analysis (see Figure 4, left). As the perturbation load increases, the buckling load decreases until a certain perturbation load P_1 is reached. Perturbation loads higher than this load do not decrease the buckling load significantly (section IV in Figure 5). The associated buckling load N_1 is defined as design load (see Figure 4, right).

Assuming a large perturbation load (e.g. $P = 10N$) the design load N_1 is approximated with one analysis. It is recommended to perform at least four buckling analyses in which the perturbation load is two times in section II and two times in section IV, (see Figure 5), to approximate the buckling load over perturbation load curve and to determine the intersection point that defines P_1 and N_1.

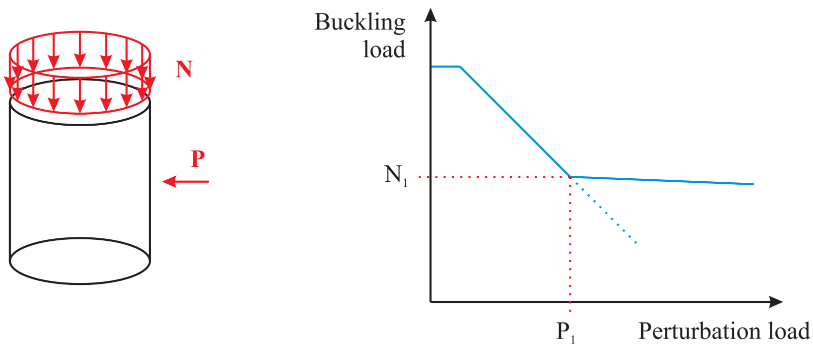

Figure 4: Concept of the single perturbation load approach

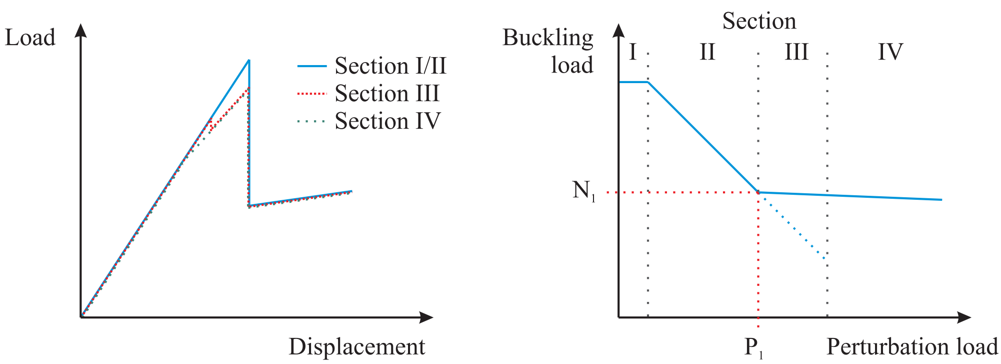

Figure 5: Sketch of load-displacement curves obtained for different perturbation load levels

The induced single buckle is the worst case geometric imperfection pattern of an axially loaded cylinder. The determined lower bound considers all geometric imperfections and other imperfections with minor influence than the geometric. However, a criterion has to be determined, for which additional imperfections an additional knockdown factor has to be applied. As shown in Table 2 the single perturbation load approach is a physical based lower boundary for all tested shells (from [Hühne (2006)]) except for shell Z12. By use of Monte Carlo simulations, it has been shown that the single perturbation load approach has a reliability of more than 99.9% for shells with geometric imperfections [Kriegesmann et al (2010a)]. This approach takes the fiber orientations from the composite shell into account and means a strong improvement compared to NASA SP-8007. If the inclination becomes a significant influence, an additional knock-down factor has to be taken into account. The size of the used inclination angle will be further investigated.

Table 2: Results of single perturbation load approach, tested shells and probabilistic analysis, from [Kriegesmann et al (2010a)]

Shell	Z07	Z09	Z10	Z12
Experimentally determined buckling load	21.8	15.7	15.7	18.6
Lower bound given by NASA SP-8007	10.2	5.5	7.4	7.1
Design load according to single perturbation load approach	17.4	14.7	13.8	20.2
99.9% quantile from Monte Carlo with only geom. Imp.	23.1	16.3	17.5	21.0
99.9% quantile from Monte Carlo including inclination	20.0	11.8	13.8	16.6

3.3 Semi-Analytic Probabilistic Analysis

For the semi-analytic probabilistic analysis used in this paper, the buckling load function $\lambda(\mathbf{x})$ is approximated by a Taylor expansion at the mean vector μ of input parameters $\mathbf{x}$. This approximation is used to estimate mean value μ_Λ and standard deviation σ_Λ of the buckling load [see e.g. Elishakoff et al (1987), Kriegesmann et al (2011)]. Taking into account only the linear terms of the Taylor expansion and assuming independence for the input parameters, the estimated mean value and variance are given by

$$\mu_\Lambda \approx \lambda(\mu) \tag{8}$$

and

$$\sigma_\Lambda^2 \approx \sum_{i=1}^{n} \left[\frac{\partial \lambda(\mu)}{\partial z_i} \right]^2 \sigma_{Z_i}^2 \tag{9}$$

where $\lambda(\mu)$ is the buckling load, evaluated and/or differentiated at the mean vector μ, z_i being the uncorrelated input parameters [by using (2)], $\sigma_{Z_i}^2$ are the variances of the input parameters. The probabilistically motivated design load λ_d is given by

$$\lambda_d = \mu_\Lambda - b\,\sigma_\Lambda \tag{10}$$

The factor b depends on the chosen level of reliability and the type of distribution. The results of this method compare well with the results of Monte Carlo simulation and with the empiric distribution [Kriegesmann et al (2011)].

Compared to the single perturbation load approach, traditional and non-traditional imperfections are taken into account. The disadvantage of this approach in contrast to the deterministic approaches is that the probabilistic design approach requires measurements of shells for which a lower bound has to be found.

3.4 Convex Anti-Optimization

The idea of convex anti-optimization is to find the combination of possible input parameters that leads to the lowest buckling load [Elishakoff (2000), Elishakof and Ohsaki (2010)]. The domain of input parameters is bounded by a hyper-ellipsoid, which encloses all measured combinations of input parameters. The buckling load function is approximated by a Taylor expansion at the center of the enclosing hyper ellipsoid $\mathbf{x}_c$ and the minimum buckling load λ_{min} can be determined as follows:

$$\lambda_{\min} \approx \lambda(\mathbf{x}_c) - \sqrt{\sum_{i=1}^{n} g_i^2 \left[\frac{\partial \lambda(\mathbf{x}_c)}{\partial \xi_i} \right]^2} \tag{11}$$

Here, g_i are the semi-axes of the ellipsoid and ξ_i are the coordinates parallel to the semi-axes. Since the minimum buckling load delivers a lower bound, it can be regarded as a design load. For the probabilistic approach as well as for the convex anti-optimization, the derivatives of the buckling load function are required, with attendant numerical evaluation.

3.5 Computational Cost

When determining the design load based on the knockdown factor concept, only the buckling load of the perfect shell has to be determined. The product of it by the KDF yields the design load.

Using the single perturbation load approach, one also needs to conduct a single buckling analysis in order to conservatively approximate N_1. For this, it must be ensured that the applied perturbation load is greater than or equal to the critical perturbation load P_1. Steinmüller et al (2008) gave an empirical estimator for P_1 for composite shells. Using this estimator, the design load is approximately determined, but conservative.

When performing a probabilistic analysis or convex anti-optimization, the partial derivatives of the buckling load must be estimated. A simple approximation of the first derivative of the buckling load function is given by

$$\frac{\partial \lambda(\mathbf{x})}{\partial x_i} \approx \frac{\lambda(x_1, \ldots, \Delta x_i + x_i, \ldots, x_n) - \lambda(\mathbf{x})}{\Delta x_i} \tag{12}$$

Hence, in order to determine the partial derivatives with respect to all n scattering input parameters, $n + 1$ buckling analyses must be performed. A more accurate estimation of the first derivative is given by

$$\frac{\partial \lambda(\mathbf{x})}{\partial x_i} \approx \frac{\lambda(x_1, \ldots, \Delta x_i + x_i, \ldots, x_n) - \lambda(x_1, \ldots, \Delta x_i - x_i, \ldots, x_n)}{2\,\Delta x_i} \tag{13}$$

which requires $2\,n + 1$ buckling analyses. The same buckling analyses results can be used to estimate the second derivatives of the buckling load function according to

$$\frac{\partial^2 \lambda(\mathbf{x})}{\partial x_i^2} \approx \frac{\lambda(x_1, \ldots, \Delta x_i + x_i, \ldots, x_n) - 2\lambda(\mathbf{x}) + \lambda(x_1, \ldots, \Delta x_i - x_i, \ldots, x_n)}{\Delta x_i^2} \tag{14}$$

With the second derivatives, the second order approaches of the probabilistic analyses and the convex anti-optimization can be performed, which are given in Kriegesmann et al (2011) and Elishakoff et al (2011).

An overview of the required number of buckling analyses for the different design procedures is given in Table 3. Using the transformation (2) for the geometric imperfections and taking into account all non-traditional imperfections yields a number of random parameters of $n = 15$.

4 Design Optimization

Using the classical knockdown factor (KDF) philosophy, optimizing the design load is equivalent to maximizing the buckling load of the perfect shell, since the KDF only scales the buckling loads. When using approaches that takes into account the change of the sensitivity within design optimization, the safety margin can be reduced significantly, which provides additional optimization potentials.

Table 3: Number of required buckling analyses for different design concepts

Design concept	Required number of buckling analyses	
	Minimum	Recommended
Knockdown Factor	1	1
Single perturbation load approach	1	1
Convex anti-optimization	$n+1$	$2\,n+1$
Semi-analytic probabilistic analysis	$n+1$	$2\,n+1$

4.1 Optimization Strategy

The goal of the following design optimization is the maximization of the design load.

For the design optimization the ply angles of the composite layers are regarded as design variables, where two cases are considered in the following. In a first step, for reasons of simplicity, visualization and comparison, the layup of four layers is restricted to be $[\pm\alpha, \pm\beta]$ (see Figure 6). In order to get the response surface of this optimization problem, the two design parameters are varied in steps of 11.25° in the interval $[0^{\circ},90^{\circ}]$ and for each combination the design load is determined.

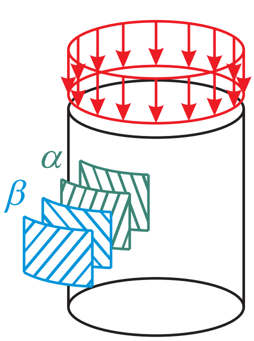

Figure 6: Maximization of buckling load by optimization of laminate setup $[\pm\alpha, \pm\beta]$

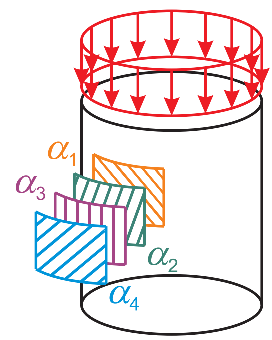

Figure 7: Maximization of buckling load by optimization of laminate setup $[\alpha_1,\alpha_2,\alpha_3, \alpha_4]$

Secondly, all four ply angles are regarded as design parameters (see Figure 7). For this optimization task, gradient based optimization methods are conducted, which requires determining the partial derivatives of the design load with respect to the design variables. The design variables are subsumed in the design vector $\mathbf{y}$ with the entries $y_1,\ldots,y_m$. The first derivative of a design load λ_d with respect to a design variable y_k can be approximated numerically by

$$\frac{\partial \lambda_d(\mathbf{y})}{\partial y_k} = \frac{\lambda_d(y_1,\ldots,\Delta y_k + y_k,\ldots,y_m) - \lambda_d(\mathbf{y})}{\Delta y_k} \tag{15}$$

This approximation requires determining the design load $m + 1$ times, where m is the number of design variables. Hence, using the methods given in section 3.3 and 3.4, $(m + 1)(n + 1)$ determinations of the buckling load are necessary per iteration step. For the single perturbation load approach, the number of required buckling analyses cannot be given in advance.

For a faster gradient based optimization, the gradients of the method given in section 3.3 and 3.4 are derived in the following. For the single perturbation load approach, no gradient based optimization is executed.

4.2 Gradient of the Probabilistically Based Design Load

Assuming the buckling load function $\lambda(\mathbf{x},\mathbf{y})$ is function of random variables, subsumed in the vector $\mathbf{x}$, and design variables, subsumed in the vector $\mathbf{y}$. Then, also the probabilistically motivated design load λ_d is a function of $\mathbf{y}$ and it is given by

$$\lambda_d(\mathbf{y}) = \mu_\Lambda(\mathbf{y}) - b\sqrt{\sigma_\Lambda^2(\mathbf{y})} \tag{16}$$

where b depends on the assumed type of distribution and the chosen level of reliability. The first derivative with respect to one design variable y_k equals

$$\frac{\partial \lambda_d(\mathbf{y})}{\partial y_k} = \frac{\partial \mu_\Lambda(\mathbf{y})}{\partial y_k} - \frac{b}{2\,\sigma_\Lambda}\frac{\partial \sigma_\Lambda^2(\mathbf{y})}{\partial y_k} \tag{17}$$

As derived in Kriegesmann (2012), the derivatives of the second order approximations of the mean value and the variance are given by

$$\frac{\partial \mu_\Lambda(\mathbf{y})}{\partial y_k} = \frac{\partial \lambda(\mu,\mathbf{y})}{\partial y_k} \tag{18}$$

and

$$\begin{aligned}\frac{\partial \sigma_\Lambda^2(\mathbf{y})}{\partial y_k} \approx\ & 2\left(\lambda_\mu - \mu_\Lambda\right)\frac{\partial \lambda}{\partial y_k} + 2\sum_{i=1}^{n}\frac{\partial \lambda}{\partial x_i}\frac{\partial^2 \lambda}{\partial x_i\,\partial y_k}\mu_{i,2} \\ & + \frac{\partial \lambda}{\partial y_k}\sum_{i=1}^{n}\frac{\partial^2 \lambda}{\partial x_i^2}\,\mu_{i,2} + \sum_{i=1}^{n}\frac{\partial^2 \lambda}{\partial x_i^2}\frac{\partial^2 \lambda}{\partial x_i\,\partial y_k}\,\mu_{i,3}\end{aligned} \tag{19}$$

If the buckling load function is assumed to be linear, the derivative of the variance vanishes and the gradient of the design load equals the gradient of the mean value.

It can be assumed that the objective function is linearly dependent of x. Then, the derivative of the variance is given by

$$\frac{\partial \sigma_\Lambda^2 (\mathbf{y})}{\partial y_k} \approx 2 \sum_{i=1}^{n} \frac{\partial \lambda}{\partial x_i} \frac{\partial^2 \lambda}{\partial x_i \, \partial y_k} \mu_{i,2} \tag{20}$$

When using this approach, it is not necessary to estimate the second derivative of the buckling load with respect to the random parameters. However, this simplification saves little computation time.

4.3 Gradient of the Design Load given by Convex Anti-Optimization

The minimum buckling load given by first order convex anti-optimization can be expressed as a function of design vector $\mathbf{y}$, is given by

$$\lambda_{\min} (\mathbf{y}) = \lambda (\mathbf{x}_c, \mathbf{y}) - \sqrt{\varphi^T (\mathbf{y}) \, \mathbf{G} \, \varphi (\mathbf{y})} \tag{21}$$

with the matrix $\mathbf{G} = diag \left(g_1^2, \ldots, g_n^2 \right)$ and the gradient of the buckling load function

$$\varphi = \left(\frac{\partial \lambda}{\partial x_1}, \ldots, \frac{\partial \lambda}{\partial x_n} \right)^T \tag{22}$$

The derivative of the minimum buckling load λ_{min} with respect to a design variable y_j equals

$$\frac{\partial \lambda_{\min}}{\partial y_j} = \frac{\partial \lambda}{\partial y_j} - \frac{1}{\sqrt{\varphi^T \mathbf{G} \, \varphi}} \, \varphi^T \, \mathbf{G} \frac{\partial \varphi}{\partial y_j} \tag{23}$$

with derivative of the gradient ϕ with respect to a design variable y_j

$$\frac{\partial \varphi}{\partial y_j} = \left(\frac{\partial^2 \lambda}{\partial x_1 \, \partial y_j}, \ldots, \frac{\partial^2 \lambda}{\partial x_n \, \partial y_j} \right)^T \tag{24}$$

5 Results

In the following sections, the results of the design optimization are given. Firstly, the design is optimized with respect to the design load given by the approaches that do not require measurement data as input, namely the knockdown factor design (see section 3.1) and the single perturbation load approach described in section 3.2. Then, the optimization results are given for the approaches presented in section 3.3 and 3.4, which take into account measurement data.

5.1 Approaches without Input of Measurement Data

Using the classical knockdown factor (KDF) philosophy, optimizing the design load is equivalent to maximizing the buckling load of the perfect shell, since the KDF only scales the buckling loads. The buckling loads of the perfect shell for different combinations $[\pm\alpha, \pm\beta]$ are given in Figure 8.

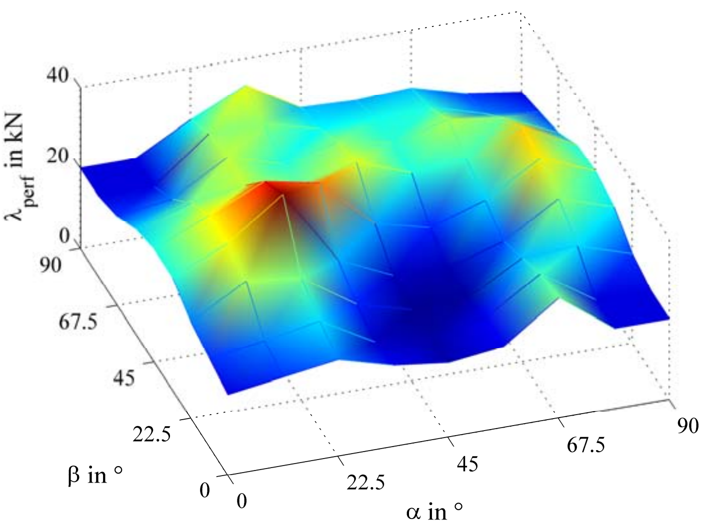

Figure 8: Buckling load of the perfect shell for different laminate setups $[\pm\alpha, \pm\beta]$

The design load according to the single perturbation load approach for different layups is shown is Figure 9. The response surfaces of the buckling load of the perfect shells as well as of the design load N_1 given by the single perturbation load approach show multiple local optima. The lay-up of the maximum buckling load of the perfect shell $[\pm 22.5^{\circ}, \pm 33.75^{\circ}]$ differs from the lay-up of the maximum design load N_1 $[\pm 22.5^{\circ}, \pm 78.75^{\circ}]$.

5.2 Approaches with Input of Measurement Data

Compared to the approaches above, the following two approaches take the strong influence of the inclination angle into account. Therefore, determining the design load given by convex anti-optimization leads to a significantly different response surface (see Figure 10) and hence, to a different optimum design.

Within the probabilistic approach the design load depends on the chosen level of reliability and the assumed type of distribution. Both are represented by the factor b

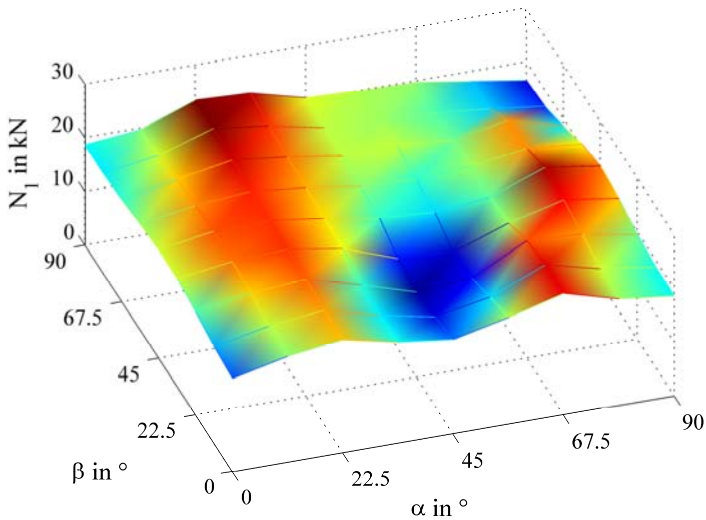

Figure 9: Design load N_1 given by single perturbation load approach for different laminate setups $[\pm\alpha, \pm\beta]$

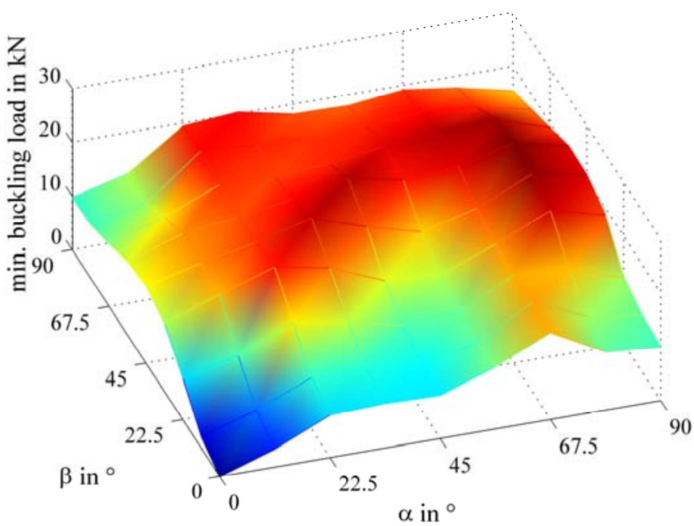

Figure 10: Design load $\lambda_{\min}$ given by convex anti-optimization for different laminate setups $[\pm\alpha, \pm\beta]$

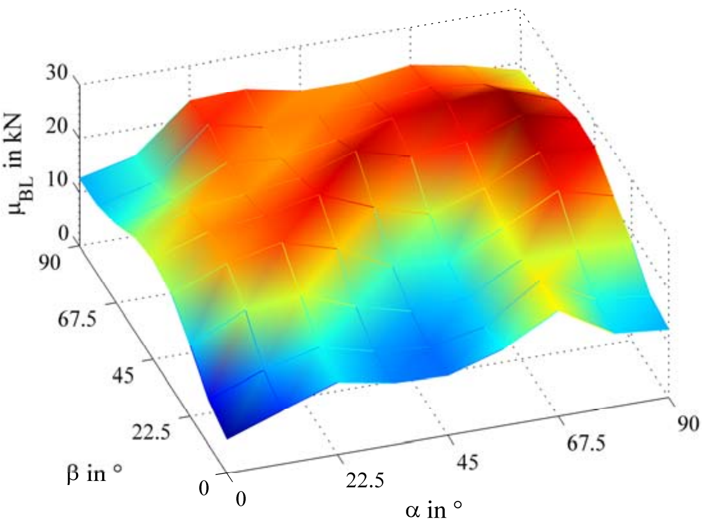

Figure 11: Mean value of buckling load for different laminate setups $[\pm\alpha, \pm\beta]$

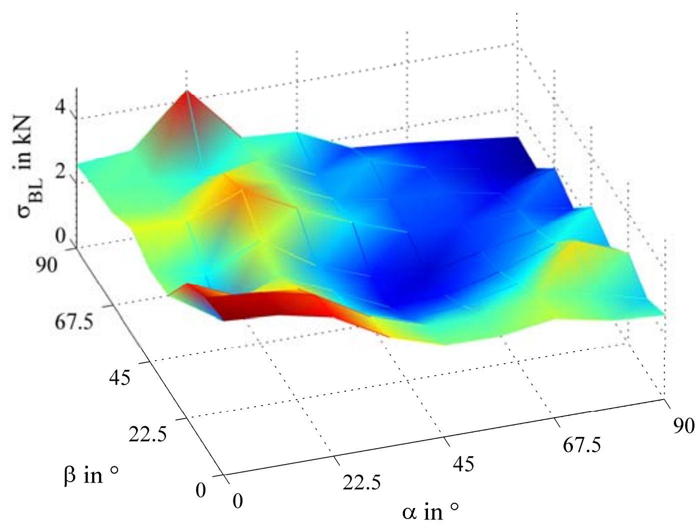

Figure 12: Standard deviation of buckling load for different laminate setups $[\pm\alpha, \pm\beta]$

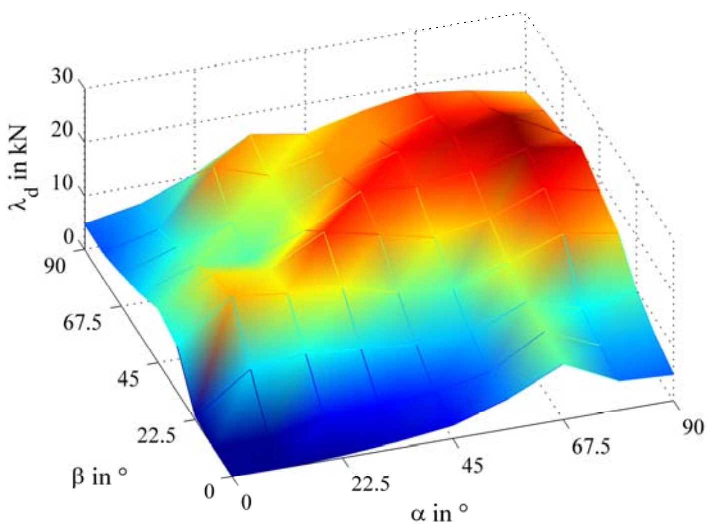

Figure 13: Design load λ_d provided by probabilistic analysis with $b = 3$ for different laminate setups $[\pm\alpha, \pm\beta]$

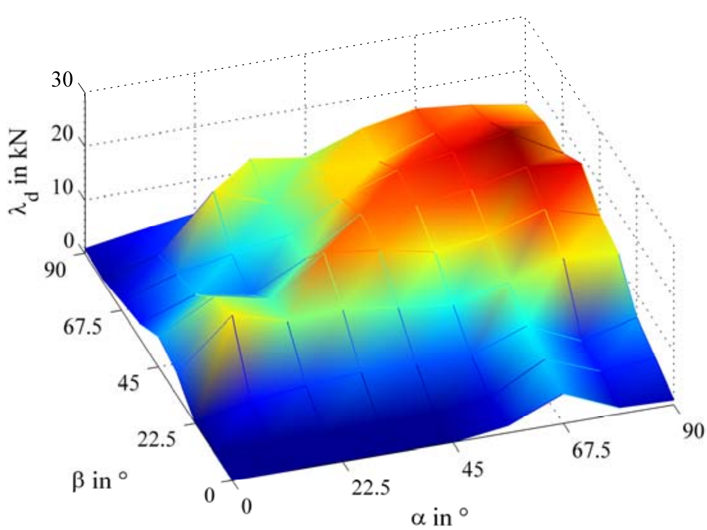

Figure 14: Design load λ_d provided by probabilistic analysis with $b = 4.5$ for different laminate setups $[\pm\alpha, \pm\beta]$

in equation (10). Hence, in a first step the mean value and the standard deviation of buckling load are determined for each different ply angle combination (see Figure 11 and Figure 12). Then, different response surfaces for different values of b are obtained according to equation (10), as plotted in Figure 13 and Figure 14.

Assuming normal distribution, $b = 3$ corresponds to a reliability of 99.87%. Within the six sigma concept [Tennant (2001)], a factor of $b = 4.5$ is typically used, for which the level of reliability equals 99.9997% assuming normal distribution. Hence, both values considered can be regarded as realistic for design purposes.

For axially stiffening layups (α and β close to zero), the design load determined from (10) is negative. Obviously, the assumption of normal distribution is not valid in these cases, but it is also obvious that the optimal design configuration cannot be found in this region. Hence, scrutinizing this area is unnecessary. It turns out that for realistic values of b the pattern of the response surface does not change significantly and the ply angle combination that leads to the maximum design load does not change. While it is a non-trivial societal and political decision, which level of reliability is acceptable, the optimal design configuration given by the probabilistic approach does not change.

Table 4: Optimal design with and without consideration of uncertainty

	Maximum design load	Optimal design
Perfect shell	43.9kN	[±22.5°, ±33.75°]
NASA SP-8007 ($\gamma = 0.322$)	14.1kN	[±22.5°, ±33.75°]
Single perturbation load approach	23.5kN	[±22.5°, ±78.75°]
Convex anti-optimization	23.3kN	[±78.75°, ±56.25°]
Probabilistic design with $b = 3$ *	23.0kN	[±78.75°, ±67.5°]
Probabilistic design with $b = 4.5$ **	20.9kN	[±78.75°, ±67.5°]

* equivalent to a reliability of 99.87%, assuming normal distribution

** equivalent to a reliability of 99.9997%, assuming normal distribution

The response surfaces of the convex anti-optimization approach and probabilistically motivated design load compare very well and lead to almost the same optimal design (see Table 4). Though the philosophies of both approaches are completely different, the good agreement appears to be not surprising. Indeed, inserting equation (8) and (9) into (10) leads to equation (25), which displays the similarities to the lower bound given by convex anti-optimization (26). For both approaches, the buckling load is evaluated and differentiated at some point in the center of the measurement vector. In both approaches, the derivatives are multiplied by some measure for the scatter of the input parameters, the standard deviation σ_{Z_i} times b

for the probabilistic approach and the semi axes g_i of the minimum volume enclosing ellipsoid for the convex anti-optimization. The products are squared, summed up and the square root of the sum is evaluated:

$$\lambda_d \approx \lambda(\mu) - \sqrt{\sum_{i=1}^{n}\left[b\,\sigma_{Z_i}\frac{\partial\lambda(\mu)}{\partial z_i}\right]^2} \tag{25}$$

$$\lambda_{\min} \approx \lambda(\mathbf{x}_c) - \sqrt{\sum_{i=1}^{n}\left[g_i\frac{\partial\lambda(\mathbf{x}_c)}{\partial\xi_i}\right]^2} \tag{26}$$

The single perturbation load approach delivers a different optimal design. The main reason for the differences between the single perturbation load approach and the probabilistic approach appears to be the boundary imperfection discussed in section 2.2. Kriegesmann et al (2010a) determined the stochastic distribution of the buckling load of four different composite shell, once taking into account the same kind of boundary imperfection as discussed in this paper, and once without taking into account any inclination. The comparison of the obtained distributions with the lower bounds given by the single perturbation load approach indicates that the single perturbation load approach covers the effect of geometric imperfections, but not of boundary imperfections completely. Since the boundary imperfection has a significant influence on the buckling load of the shells considered, the range of the design load given by the single perturbation load approach is smaller than the range of design loads given by probabilistic approach and the convex anti-optimization. However, the response surfaces of single perturbation load approach and convex anti-optimization show similarities, as there are local maxima for [$\pm 22.5^\circ$, $\pm 78.75^\circ$] and a local minimum around [$\pm 45^\circ$, $\pm 22.5^\circ$].

The response surface of the perfect shell analysis differs significantly from the procedures that incorporate uncertainties and leads to a design that is sensitive to scattering input parameters, according to the probabilistic analysis. Furthermore, the maximum design load given by the KDF procedure is much more conservative than the maximal design loads obtained from all other approaches considered.

For the probabilistic design load and the design load given by convex anti-optimization, optimal design is determined using a gradient based algorithm. Starting from the optimum found in the optimization by stepwise variation of the ply angles, the optimal design configuration and the associated design load given in Table 5 are obtained. The optimal designs as well as the design load hardly differ from the one found by stepwise variation of the ply angles. This result is not surprising when looking at the response surface of this problem (see Figure 10 and Figure 13). However, it cannot be stated definitely, that there is no better design configuration when treating all four ply angles independently as design variables. It is possible that for a different start of the gradient based optimization a higher design load can be found. However, though several initial guesses has been tested, no higher design load has been found in the context of this work.

Table 5: Results of the gradient based optimization of cylindrical shells under uncertainty

	Maximum design load	Optimal design
Convex anti-optimization		
with 2 design variables	23.74 kN	[±79.4°, ±56.8°]
with 4 design variables	23.78 kN	[84.1°, -75.2°, 57.5°, -55.5°]
Probabilistic design with b = 3		
and 2 design variables	22.16 kN	[±78.1°, ±66.9°]
and 4 design variables	23.00 kN	[78.4°, -78.1°, 66.2°, -67.6°]

6 Conclusions

Different design approaches for axially compressed cylindrical shells have been described and applied to composite shells. The design loads given by the different design procedures have been maximized by optimizing the laminate setup. The KDF concept provides a very conservative design load. Maximizing the design load given by the knockdown factor concept is equivalent to maximizing the buckling load of the perfect shell. Therefore, imperfection sensitivity is not considered within this approach and the optimization yields an imperfection sensitive design.

In case no imperfection measurements are available for the shells considered, the single perturbation load approach is a promising basis for optimization, since this method does not require imperfection data. The reduction of the buckling load by geometric imperfections is taken into account. Further imperfections like the inclination angle with a significant influence has to be taken into account by an additional knockdown factor. The size of the inclination angle has to be still further investigated. Taking the inclination angle into account in the convex anti-optimization and probabilistic approach the optimal design differs from the one found with the single perturbation load approach. However, the response surfaces show significant similarities. Furthermore, the design loads of the optimal designs given by these three approaches compare very well. The convex anti-optimization approach and the probabilistic approach, which both take into account measured imperfection data, deliver similar response surfaces within the optimization and lead to almost the same optimal design. The convex anti-optimization approach implies the assumption that the measurement data are bounded by a hyper ellipsoid, which cannot be verified. Compared to the probabilistic approach, convex anti-optimization does not require choosing a level of reliability and a type of distribution. However, within the present probabilistic design optimization, the assumed type of distribution and the chosen level of reliability have no influence on the optimal design configuration.

References

Arbocz, J., Hol, J. M. A. M. (1991): Collapse of Axially Compressed Cylindrical Shells with Random Imperfections, *AIAA Journal*, vol. 29, no. 12, pp. 2247–2256.

Arbocz, J., Stam, A. R. (2004): A Probabilistic Approach to Design Shell Structures, in *Buckling of Thin Metal Shells (J. G. Teng and J. M. Rotter, eds.)*, London: Spon Press, pp. 455–489.

Arbocz, J., Starnes Jr, J. H. (2002): Future Directions and Challenges in Shell Stability Analysis, *Thin-Walled Structures*, vol. 40, no. 9, pp. 729–754.

Degenhardt, R., Kling, A., Bethge, A., Orf, J., Kärger, L., Zimmermann, R., Rohwer, K., and Calvi, A. (2010): Investigations on Imperfection Sensitivity and Deduction of Improved Knock-down Factors for Unstiffened CFRP Cylindrical Shells, *Composite Structures*, vol. 92, no. 8, pp. 1939–1946.

DeVries, J. (2009): The Imperfection Data Bank and its Applications, TU Delft dissertation, Delft.

ECCS (1988): Buckling of Steel Shells: European recommendations, Brussels, Belgium, ECCS 56.

Elishakof, I. and Ohsaki, M. (2010): *Optimization and Anti-Optimization of Structures Under Uncertainty*. Imperial College Press.

Elishakoff, I. (1983): How to Introduce Initial-Imperfection Sensitivity Concept into Design, in *Collapse: The Buckling of Structures: Theory and Practice (J. M. T. Thompson and G. W. Hunt, eds.)*, Cambridge, UK: Cambridge University Press, pp. 345–357.

Elishakoff, I., van Manen, S., Vermeulen, P. G., Arbocz, J. (1987): First-Order Second-Moment Analysis of the Buckling of Shells with Random Imperfections, *AIAA journal*, vol. 25, no. 8, pp. 1113–1117.

Elishakof, I. (1998): How to Introduce Initial-Imperfection Sensitivity Concept into Design 2, NASA SP-1998-206280.

Elishakoff, I. (2000): Uncertain Buckling: Its Past, Present and Future, *International Journal of Solids and Structures*, vol. 37, no. 46–47, pp. 6869–6889.

Elishakoff, I. (2012): Probabilistic Resolution of the Twentieth Century Conundrum in Elastic Stability, **Thin-Walled Structures**, vol. 59, pp. 35–57.

Elishakoff, I., Li, Y., Starnes, J. H. (2001): *Non-Classical Problems in the Theory of Elastic Stability*. Cambridge: Cambridge University Press.

Elishakoff, I., Kriegesmann, B., Rolfes, R., Hühne, C., and Kling, A. (2011): Optimization and Anti-Optimization of Buckling Load for Composite Cylindrical Shells under Uncertainties, *AIAA Journal*, vol. 50, no. 7, pp. 1513-1524.

Eurocode 3 (2002): General Rules: Strength and Stability of Shell Structures, Brussels, Belgium, Eurocode 3 Part 1.6.

Hilburger, M. W. and Starnes Jr, J. H. (2002): Effects of Imperfections on the Buckling Response of Compression-Loaded Composite Shells, *International Journal of Non-Linear Mechanics*, vol. 37, no. 4–5, pp. 623–643.

Hühne, C., Rolfes, R., Breitbach, E., Tebmer, J. (2008): Robust Design of Composite Cylindrical Shells Under Axial Compression – Simulation and Validation, *Thin-Walled Structures*, vol. 46, no. 7–9, pp. 947–962.

Hühne, C. (2006): Robuster Entwurf beulgefährdeter, unversteifter Kreiszylinderschalen aus Faserverbundwerkstoff, Forschungsbericht 2006-17, ISSN 1434-8454, Deutsches Zentrum für Luft- und Raumfahrt,

Kriegesmann, B., Rolfes, R., Hühne, C., Tessmer, J. and Arbocz, J. (2010a): Probabilistic Design of Axially Compressed Composite Cylinders with Geometric and Loading Imperfections, *Int. J. Str. Stab. Dyn.*, vol. 10, no. 4, pp. 623–644.

Kriegesmann, B., Rolfes, R., Hühne, C., and Kling, A. (2010b): Probabilistic Second-Order Third-Moment Approach for Design of Axially Compressed Composite Shells, in *Proceedings of the 51st AIAA/ASME/ASCE/AHS/ASC Structures, Structural Dynamics, and Materials Conference*, Orlando, Florida, USA, pp. AIAA–2010–2534.

Kriegesmann, B., Rolfes, R., Hühne, C., and Kling, A. (2011): Fast Probabilistic Design Procedure for Axially Compressed Composite Cylinders, *Composites Structures*, vol. 93, pp. 3140–3149.

Kriegesmann, B. (2012): Probabilistic Design of Thin-Walled Fiber Composite Structures, Leibniz University Hannover dissertation, Hannover, Germany.

NASA (1968): Buckling of Thin-Walled Circular Cylinders, NASA SP-8007.

Orf, J. (2008): Einfluss von Imperfektionen auf das Beulverhalten unversteifter CFK-Zylinder, Bauhaus-University Weimar, Institut für Strukturmechanik, Diplomarbeit.

DIN 18800 (1990): Stahlbauten – Stabilitätsfälle, Schalenbeulen, Berlin, DIN 18800 Teil 4.

Steinmüller, P., Degenhardt, R., Rohwer, K. (2008): Investigations of Axially Loaded Unstiffened CFRP Cylindrical Shells Subject to Single Perturbation Loads, presented at the 2nd International Conference on Buckling and Postbuckling Behaviour of Composite Laminated Shell Structures with COCOMAT Workshop, Braunschweig, Germany.

Tennant, G. (2001): *Six Sigma: SPC and TQM in manufacturing and services*. Gower Publishing, Ltd.

Weingarten, V. I., Morgan, E. J. and Seide, P. (1965): Elastic Stability of Thin-Walled Cylindrical and Conical Shells Under Axial Compression, *AIAA Journal*, vol. 3, no. 3, pp. 500–505.

Zimmermann, R. (1992): Optimierung axial gedrückter CFK-Zylinderschalen, VDI Verlag, Fortschritt-Berichte VDI, Reihe 1, Fortschritt-Berichte VDI 207.